Casimir effects for a flat plasma sheet: I. Energies

2005 J. Phys. A: Math. Gen. 38 2997

(http://iopscience.iop.org/0305-4470/38/13/013)

INSTITUTE OF PHYSICS PUBLISHING JOURNAL OF PHYSICS A: MATHEMATICAL AND GENERAL

J. Phys. A: Math. Gen. **38** (2005) 2997–3019 doi:10.1088/0305-4470/38/13/013

Casimir effects for a flat plasma sheet: I. Energies

G Barton

Department of Physics and Astronomy, University of Sussex, Brighton BN1 9QH, UK

Received 19 October 2004, in final form 5 January 2005
Published 14 March 2005
Online at stacks.iop.org/JPhysA/38/2997

Abstract

We study a fluid model of an infinitesimally thin plasma sheet occupying the xy plane, loosely imitating a single base plane from graphite. In terms of the fluid charge e/a^2 and mass m/a^2 per unit area, the crucial parameters are $q \equiv 2\pi e^2/mc^2a^2$, a Debye-type cutoff $K \equiv \sqrt{4\pi}/a$ on surface-parallel normal-mode wavenumbers k, and $X \equiv K/q$. The cohesive energy β per unit area is determined from the zero-point energies of the exact normal modes of the plasma coupled to the Maxwell field, namely TE and TM photon modes, plus bound modes decaying exponentially with $|z|$. Odd-parity modes (with $E_{x,y}(z = 0) = 0$) are unaffected by the sheet except for their overall phases, and are irrelevant to β, although the following paper shows that they are essential to the fields (e.g. to their vacuum expectation values), and to the stresses on the sheet. Realistically one has $X \gg 1$, the result $\beta \sim \hbar cq^{1/2}K^{5/2}$ is nonrelativistic, and it comes from the surface modes. By contrast, $X \ll 1$ (nearing the limit of perfect reflection) would entail $\beta \sim -\hbar cqK^2 \log(1/X)$: contrary to folklore, the surface energy of perfect reflectors is divergent rather than zero. An appendix spells out the relation, for given $\mathbf{k}$, between bound modes and photon phase-shifts. It is very different from Levinson's theorem for 1D potential theory: cursory analogies between TM and potential scattering are apt to mislead.

PACS numbers: 03.65.−w, 03.70.+k, 11.10.−z, 12.20.−m, 36.40.Gk, 42.50.Pq

1. Introduction

1.1. Background and motivation

By Casimir effects one commonly understands the consequences of changes in the quantized Maxwell field due to the introduction of macroscopic bodies described merely by their geometry and by their classical electromagnetic response functions. For stationary bodies such effects are conveniently classified into two main types. The first type embraces forces between disjoint bodies: spectacular recent advances in experimental techniques have brought

these to the forefront also of theoretical research, where, apart from ongoing arguments about nonzero temperatures, the basic principles are no longer in serious question. (See the review by Bordag *et al* (2001); later references can be traced for instance from Genet *et al* (2003) and from Reynaud *et al* (2004).)

Problems of the second type concern the energy (and eventually the internal stresses) of a single body. These questions have long been bedevilled by confusion flowing from their original focus on material shaped into a spherical shell and treated as infinitesimally thin but perfectly reflecting (Boyer 1968): a scenario from which it has taken surprisingly long to progress to theories capable of accommodating less unrealistically modelled media. For the Maxwell field in the presence of dispersive reflectors, a start has now been made along the lines of what is traditionally called *nonrelativistic quantum electrodynamics*: perturbatively for insulators of several simple shapes (Barton 2001a, 2001b, 2002, Marachevsky 2001a, 2001b), and exactly for an infinitesimally thin spherical plasma shell (Barton 2004a, 2004b, referred to as B.III and B.IV). The physics of this plasma model, and a critique of older approaches, are spelled out in B.III. So is a concordance with recent studies of the relations between Casimir effects and the standard renormalization theory of quantized fields (for scalar fields coupled to passive potentials, though not as yet for the Maxwell field). This work may be traced through, say, Graham *et al* (2004).

However, the quantum physics of such plasmas is more readily appreciated if one explores also the simpler problem of the same sheet left flat and indefinitely extended; the more so because the results emerge in closed form, and unobscured by the technical difficulties of Bessel functions that are unavoidable for spheres. The present paper (B.V, projected on p 1016 of B.III) does just that as regards *the cohesive energy* β per unit area. For understanding the structure of this kind of Casimir problem more generally, perhaps the most important lesson is that β is indeed the energy of primary physical interest; that there is a fairly straightforward strategy for calculating it; that the calculation automatically focuses attention on the dominant parts of β; which then identifies as physically secondary (though mathematically fascinating) the traditional preoccupations induced by observing that for spherical shells of radius R the combination $\hbar c/R$ has the dimensions of energy, without featuring any material constants. This accidental fact, without a significant analogue for β (cf section 3.5), can then tempt one to mis-identify the total cohesive energy B of the sphere as that (relatively unimportant) component of B which is indeed proportional to $\hbar c/R$, with the very confusing consequences discussed in B.III.

The following paper (Barton 2005, referred to as B.VI) spells out what the model entails for the quantized fields, in particular for their ground-state (vacuum) expectation values as functions of distance z from the sheet. The connections with β are surprisingly subtle: for instance, the mean-square fields, measurable at least in principle, include crucial contributions that are nevertheless irrelevant to β because they stem from the self-energies of the charge carriers.

It is worth stressing that, very deliberately, we work only with the fields: potentials are not needed and are not introduced[1], so that gauge-independence is never in question.

Meant as they are chiefly for preliminary orientation, both this paper and B.VI are restricted to a plasma sheet without internal dissipation (e.g. without ohmic losses), and at zero temperature. To relax the first restriction one would elaborate the model along the lines of Huttner and Barnett (1992) and of Barnett *et al* (1996) (for recent references see e.g. Suttorp and Wubs (2004)); and both restrictions would need to be relaxed before the model could

[1] Except in section 4 of B.VI, which considers the interaction between the sheet and a charged particle.

hope to illuminate the currently vexed question of the temperature dependence of the Casimir attraction between two parallel sheets some finite distance apart.

1.2. Preview and summary

Section 2.1 is a brief sketch of our model as adapted to a flat sheet: most of the basic physics was discussed in B.III, albeit *à propos* of a spherical shell. For as long as possible we deal with a continuous fluid mimicking a number $n \equiv 1/a^2$ of charge carriers per unit area, with charge ne and mass nm per unit area. However, as B.III also explained, physically sensible results for cohesive energies emerge only if one imposes a Debye-type cutoff $K = \sqrt{4\pi}/a$ on wave-numbers k parallel to the sheet, motivated in standard fashion by the granularity of the true underlying material. Further, equation (2.5) will identify a dimensionless parameter $X = amc^2/e^2\sqrt{\pi}$, whose inverse turns out to measure the effective coupling strength between fields and plasma: $X \gg 1$ indicates weak coupling (the realistic option), while $X \ll 1$ would, formally, indicate strong coupling, albeit $X \to 0$ is in fact incompatible with our basic assumption that the plasma moves nonrelativistically.

The same section defines the nonretarded (NR), the perfectly-reflecting (PR) and the no-cutoff (NC) limits. The NR limit yields the energies to leading order; it can be accessed directly through the *nonretarded model* (appendix B); and it is the only limit relevant to the present paper. The PR limit (incompatible with the NR) is in the writer's experience confusing more often than helpful, but for historical reasons one cannot safely ignore it altogether. It and some of the prima-facie paradoxes attending it are discussed in appendix F of B.VI. The NC limit makes no sense for energies, and plays no role in the present paper. By contrast, on the fields (eg on their mean squares) it is doubtful whether a cutoff should be imposed at all, seeing that they necessarily include the self-fields. Paper B.VI discusses this question further, and will in fact proceed without a cutoff, except in some appendices which illustrate the effects a cutoff would have if one imposed it with one's eyes closed.

Section 2.2 writes the equations of motion (Maxwell's for the fields and Newton's second law for the plasma); identifies the transverse-electric (TE) and transverse-magnetic (TM) reflection and transmission coefficients and phase shifts of the continuum (photon) modes; and determines the normal modes of definite parity, including the surface-bound (surface plasmon) modes, which are pure TM, and have sharp frequencies $\Omega(k)$. (The relation between phase shifts and bound modes is pursued further in appendix A.)

Section 3 then determines the (in principle) observable cohesive energy β from the surface-mode eigenfrequencies Ω and from the photon phase shifts: β requires no other information about the normal modes. It is crucially important that to obtain β from the total ground-state energy, one must exclude both the zero-point energy of the Maxwell field in the absence of the sheet, and also the self-energy of the charge carriers. The first subtraction is familiar and almost automatic; the second features the Born approximation to the phase shifts. To leading order in $1/X$, β agrees as it should with $B/4\pi R^2$, where B (calculated in B.III) is the total cohesive energy of a spherical shell having radius R.

The various contributions to β are specified by various dimensionless functions $\mathcal{L}(X)$. Exact closed expressions are given in sections 3.2 and 3.3, and relatively transparent asymptotic approximations in section 3.4. Figures 1–4 indicate how the $\mathcal{L}$ vary between the asymptotic regimes. Section 3.4 also exorcises (once again) the old delusion that the surface energy β vanishes in the PR limit.

The energy β resides partly in the fields, i.e. off the sheet, and partly on the sheet as the mean kinetic energy κ of the charge carriers. Section 4 determines κ, requiring far more detailed information about the normal-mode amplitudes than was needed for β.

Tables 1 and 2 and figure 5 compare the scaling functions $\mathcal{L}$ with their analogues $\mathcal{K}$ for κ. In particular, table 1 shows that for weak coupling one has $\kappa \simeq \beta/2$ for the dominant surface-plasmon and thereby for the overall energies, as suggested by the virial theorem for the essentially nonrelativistic surface-mode oscillators; but that the ratios are very different for the (subdominant) contributions from the photon modes. Finally section 4.3 shows that $X \to 0$ indeed makes κ comparable to the rest energy of the charge carriers, confirming that their motion has become relativistic.

Appendix A compares the relations between bound and continuum modes in our electromagnetic scenario (for given k) with those from 1D potential scattering. In both cases, the bound modes locate the poles of the transmission and reflection amplitudes in the complex plane of frequency or of perpendicular wave-number p. But potential and TM scattering differ sharply regarding the change in the phase shift as the frequency or as p rise from threshold to infinity. In potential theory, Levinson's theorem derives this change from the fact that every bound state is formed from a continuum state attracted below threshold, so that the total number of states is unaffected by the potential. But in our plasma model a careful count shows that the TM continuum holds exactly as many modes with as without the sheet. In other words, the bound mode is additional to the continuum modes, compatibly with the fact that it exists also in the NR model, which has no continuum to begin with. By contrast, for TE polarization the analogy with potential theory is complete. These observations will be presented merely as isolated mathematical facts: the writer knows of no systematic extension of Levinson's theorem to electromagnetism. It might prove an interesting problem, if only because misconceived analogies with potential scattering have led some arguments badly off the rails.

Finally, we risk the obvious to say that our model is designed for a preliminary exploration of the consequences of dispersion in Casimir problems, without in any way meaning to pre-empt calculations on materials modelled differently. In particular, inferences drawn from the general pattern of our results are subject to caution on dimensional grounds: here, the important combination $(ne)^2/(nm) = ne^2/m$ has the dimensions $[L^{-1}T^{-2}]$, in contrast to 3D plasmas which instead of n feature a volume density n', so that $[n'e^2/m] = [T^{-2}]$, with $4\pi n'e^2/m$ the familiar squared plasma frequency.

2. The model

2.1. The hydrodynamic model

We start with a brief outline of the model introduced in B.III, designed as a loose imitation of a single base-plane in graphite. It posits an infinitesimally thin and indefinitely extended flat sheet occupying the xy-plane, carrying a continuous fluid with mass and charge densities nm, ne per unit area, plus an immobile, uniformly distributed, overall-neutralizing background charge[2]. The subscript $\parallel$ indicates vector components parallel to the sheet, and $\mathbf{r} = (\mathbf{s}, z)$, i.e. $\mathbf{s} = \mathbf{r}_\parallel = (x, y)$. The fluid displacement $\boldsymbol{\xi}$ is purely tangential, with surface charge and current densities

$$\sigma = -ne\boldsymbol{\nabla}_\parallel \cdot \boldsymbol{\xi}, \qquad \mathbf{J} = ne\dot{\boldsymbol{\xi}}. \tag{2.1}$$

[2] One improvement would introduce fluid pressure as a function of density (ie spatial dispersion). Another would replace the fluid with a 2D Fermi gas (Fetter 1973), which however would thoroughly de-emphasize and probably obscure the features of most interest to quantum electrodynamics generally, and to Casimir effects in particular.

The motion is assumed to be nonrelativistic ($\dot{\xi} \ll c$), so that the Lorentz force is negligible, and Newton's second law reads[3]

$$\partial^2 \boldsymbol{\xi}(s,t)/\partial t^2 = (e/m)\mathbf{E}_{\|}(\mathbf{s}, z=0, t). \tag{2.2}$$

Evidently the model mimics *n delocalized* particles per unit area, call them electrons, each with charge and mass e, m. The surface density n is related to some mean inter-electron distance a by

$$n \equiv 1/a^2.$$

Merely for orientation, we shall form rough estimates with a of the order of a few Bohr radii, far longer than the classical electron radius r_0:

$$a \sim a_B \equiv \hbar^2/me^2, \qquad r_0 \equiv e^2/mc^2, \qquad r_0/a \sim (e^2/\hbar c)^2 \equiv \alpha \simeq (1/137)^2, \tag{2.3}$$

using unrationalized Gaussian units.

Moreover, we impose *a Debye-type cutoff K* on the surface-parallel wavenumbers of waves that the fluid can support, and by the same token also on Maxwell waves that can interact effectively with the fluid as such (as distinct from the individual charge carriers out of which in the last analysis the fluid is formed). Paper B.III motivates and discusses the physics of the cutoff in some detail. Thus,

$$\pi K^2/(2\pi)^2 \equiv n \quad \Rightarrow \quad K = \sqrt{4\pi}/a. \tag{2.4}$$

The no-cutoff limit considered later would break this link by letting $K \to \infty$ with all other parameters fixed, including a.

By hindsight we define another characteristic wavenumber $q \equiv (2\pi/c^2)(ne)^2/(nm)$, and observe that the input parameters of the model (ne, nm, K, and through Maxwell's equations also c) admit only one dimensionless combination[4] X:

$$q \equiv 2\pi ne^2/mc^2 = 2\pi n r_0, \qquad X \equiv K/q = a/r_0\sqrt{\pi} \sim 1/\alpha^2 \gg 1. \tag{2.5}$$

It will emerge presently that $1/X$ is, effectively, a coupling-strength parameter: $X \gg 1$ means that the interaction between fields and fluid is weak, and $X \ll 1$ means that it is strong (see e.g. (2.14)–(2.16)).

Regarding dimensions, we anticipate to stress that, as zero-point expectation values, all our results for energies and mean-square fields are automatically and explicitly proportional to $\hbar$; and that, conversely, $\hbar$ enters in no other way. Thus we meet no true expansions by powers of α, which can feature only accidentally. That is what has happened for instance in (2.5), simply through our choice, in (2.3), of the Bohr radius as our estimate of a.

Likewise it will prove useful to keep track of powers of c. In particular, noting that $q \sim 1/c^2$ and $X \sim c^2$, we stress by hindsight that, dimensionally,

$$\left[\frac{\text{energy}}{\text{area}}\right] = [\hbar c q^3], \qquad \hbar c q^3 X^{5/2} = \hbar c q^{1/2} K^{5/2} = \hbar\sqrt{\frac{2\pi ne^2}{m}}\,K^{5/2}, \tag{2.6}$$

$$\left[\frac{\text{energy}}{\text{volume}}\right] = [\mathbf{E}^2] = [\mathbf{B}^2] = [\hbar c q^4], \qquad \hbar c q^4 X^{7/2} = \hbar c q^{1/2} K^{7/2} = \hbar\sqrt{\frac{2\pi ne^2}{m}}\,K^{7/2}, \tag{2.7}$$

the second relation in each line indicating the unique combination that is independent of c.

[3] We shall study only small-amplitude oscillations. Uniform flow (strictly constant $\dot{\boldsymbol{\xi}}$) is excluded: though it might seem reasonable for a fluid model taken literally, it is totally unrealistic for the kind solid-state plasmas that we have in mind.

[4] The reader is due an apology for the fact that X in this paper is not the same as the combination R/a which was called X in B.III and B.IV. Further, what here we call strong coupling in virtue of $X \ll 1$ corresponds to what B.III (p 1013) called strong coupling in virtue of $x \equiv e^2/mc^2a \gg 1$ at fixed R; the flat sheet has no analogue to what B.III called strong coupling in virtue of $R/a \gg 1$ at fixed x.

Finally, we list three widely considered limits which, though often deceptive, can on other occasions highlight important features of the more complicated exact results.

- *The nonretarded (NR) limit*. $c \to \infty$ at fixed a and K, entailing $q \to 0$, with $c\sqrt{q}$ fixed and finite, and $X \to \infty$. The *nonretarded model* (appendix B) implements the limit from the start: then there are no photons, and the only excitations of the sheet are surface plasmons. It yields the far and away dominant component of β, unsurprisingly to the condensed-state physicist, who has always known that the cohesive energy of more or less ordinary solids is given to an excellent approximation without reference to Maxwell's equations or to quantum electrodynamics.
- *The perfect-reflector (PR) limit*, designed to make the sheet reflect perfectly at all frequencies, which will be seen presently to require $q \to \infty$. This can be envisaged in at least two different ways, bearing in mind that $K \sim 1/a$ and $X = K/q \sim a/r_0$: either (i) $a \to 0$ at fixed r_0, so that $K \to \infty$; or (ii) $r_0 \to \infty$ at fixed a and therefore fixed K. It proves important that in both cases $X \to 0$. Though section 4.3 shows that *very* small X is incompatible with our basic assumption that $\dot{\xi} \ll c$, it also suggests that values down to $X \sim 0.1$, though certainly fanciful, might not be intrinsically absurd.
- *The no-cutoff (NC) limit* is artificial in that itabandons the Debye connection between a and K, and contemplates $K \to \infty$ at fixed a and fixed q, which would also entail $X \to \infty$. Section 1.2 has already warned that this limit is inadmissible as regards energies. On the other hand, cutoffs are inappropriate to the fields, and B.VI will proceed without one except occasionally for illustration.

Reverting briefly to the PR limit, and anticipating section 2.2, we anticipate also that in a formal sense the approach to this limit appears to present a paradox, because it forces one to reconcile the two apparently conflicting facts that (i) the odd-parity modes are totally indifferent to how the sheet reflects; while (ii) in the limit, a perfectly reflecting sheet turns the half-spaces with $z \lessgtr 0$ into electromagnetically independent systems, each having its own Hilbert space, with the overall Hilbert space just the direct product of the two. Since this problem bears primarily on the fields rather than on the energies, we postpone more detailed discussion to B.VI, appendix E.2.

2.2. Maxwell's equations and the normal modes

For normal modes, with all time variation described by a common factor $\exp(-\mathrm{i}\omega t)$, equation (2.2), and Maxwell's equations plus (2.1), read

$$\boldsymbol{\xi} = -(e/m\omega^2)\mathbf{E}_\parallel, \qquad \mathbf{J} = -\mathrm{i}\omega ne\boldsymbol{\xi}, \qquad \sigma = -ne\boldsymbol{\nabla}_\parallel \cdot \boldsymbol{\xi}, \tag{2.8}$$

$$\boldsymbol{\nabla} \cdot \mathbf{B} = 0, \qquad \boldsymbol{\nabla} \times \mathbf{E} - \mathrm{i}\omega\mathbf{B}/c = 0, \tag{2.9}$$

$$\boldsymbol{\nabla} \cdot \mathbf{E} = 4\pi\delta(z)\sigma, \qquad \boldsymbol{\nabla} \times \mathbf{B} + \mathrm{i}\omega\mathbf{E}/c = 4\pi\delta(z)\mathbf{J}/c. \tag{2.10}$$

To obtain the matching conditions on the fields, we integrate equations (2.10) across the sheet, which amounts to applying Gauss' law and Ampère's law. They yield

$$\mathrm{discont}(\mathbf{E}_\parallel) = 0, \qquad \mathrm{discont}(E_z) = 2q(c/\omega)^2\boldsymbol{\nabla}_\parallel \cdot \mathbf{E}_\parallel, \tag{2.11}$$

$$\mathrm{discont}(B_z) = 0, \qquad \mathrm{discont}(\mathbf{B}_\parallel) = -\mathrm{i}2q(c/\omega)\hat{\mathbf{z}} \times \mathbf{E}_\parallel, \tag{2.12}$$

equations that determine the normal modes, and mathematically speaking define the model.

To describe the normal modes we introduce the two-component surface-parallel wavevector $\mathbf{k}$, and the surface-normal wave-number p, defined to be strictly non-negative (so as to avoid redundancy); and, for continuum (ie for photon) modes, their frequency ω:

$$p \geqslant 0, \qquad \omega = c\sqrt{k^2 + p^2} \qquad \text{(photons)}. \tag{2.13}$$

The two polarizations are chosen as TE (with $E_z = 0$) and TM (with $B_z = 0$). Then the reflection and transmission amplitude-ratios (which do not enter our calculations directly) read

$$\mathcal{R}^{\mathrm{TE}} = \frac{-\mathrm{i}q}{p + \mathrm{i}q} = \mathrm{i}\sin(\eta)\,\mathrm{e}^{\mathrm{i}\eta}, \qquad \mathcal{T}^{\mathrm{TE}} = \frac{p}{p + \mathrm{i}q} = \cos(\eta)\,\mathrm{e}^{\mathrm{i}\eta}, \tag{2.14}$$

$$\mathcal{R}^{\mathrm{TM}} = \frac{-\mathrm{i}qp}{k^2 + p^2 + \mathrm{i}qp} = \mathrm{i}\sin(\mu)\,\mathrm{e}^{\mathrm{i}\mu}, \qquad \mathcal{T}^{\mathrm{TM}} = \frac{k^2 + p^2}{k^2 + p^2 + \mathrm{i}qp} = \cos(\mu)\,\mathrm{e}^{\mathrm{i}\mu}, \tag{2.15}$$

featuring the phase shifts η and μ, with

$$\tan\eta(p) = -q/p, \qquad \tan\mu(p,k) = -c^2qp/\omega^2 = -qp/(k^2 + p^2). \tag{2.16}$$

The S matrices for given $\mathbf{k}$ are $\exp(2\mathrm{i}\eta)$ and $\exp(2\mathrm{i}\mu)$.

The phase shifts are chosen to vanish as $p \to \infty$, so that $\eta(p = 0) = -\pi/2$, while $\mu(p = 0, k \neq 0) = 0$. Appendix A examines this threshold behaviour in the light of Levinson's theorem. Meanwhile we note only that at $p = 0$ the $\mathcal{R}, \mathcal{T}$ can be determined almost trivially; and that there is nothing paradoxical about $\mathcal{R}^{\mathrm{TM}} = 0$ and $\mathcal{T}^{\mathrm{TM}} = 1$ (not even though in potential scattering this scenario, described as a transmission resonance at threshold, would be highly exceptional). Excitations with $p = 0$ are plane waves running parallel to the sheet, say in the x-direction. (i) The plane-polarized wave with $\mathbf{E} = \hat{y}E$ parallel to the sheet, ie TE, must have $\mathbf{B} = \hat{\mathbf{z}}B$. In general such an $\mathbf{E}$ induces a current in the sheet, which by Ampère's theorem requires a finite discontinuity in the y component of $\mathbf{B}$. Since $\mathbf{B}$ has no such component, this is impossible, and contradiction can be avoided only if $E(z = 0)$ vanishes. Formally speaking, that is precisely what is achieved by perfect reflection. But in point of physical fact $\mathcal{R} = -1$ and $\mathcal{T} = 0$ combined with $p = 0$ mean that all the fields vanish everywhere, so that the presence of the sheet makes it impossible to excite such waves in the first place. In other words, since the scenario cannot be realized, it can generate no paradoxes[5].

(ii) The other plane-polarized wave, with $\mathbf{B} = \hat{\mathbf{y}}B$, i.e. TM, must have $\mathbf{E} = \hat{\mathbf{z}}E$; therefore it cannot affect the sheet at all, whence the sheet cannot affect the wave, which means precisely $\mathcal{R} = 0$ and $\mathcal{T} = 1$, as indicated by (2.15) and (2.16).

For our purposes the normal modes are conveniently classified according to the parity ($\pm$) of $\mathbf{E}_\parallel$. Equation (2.2) shows that the odd-parity modes do not interact with the sheet, because they have $\mathbf{E}_\parallel(z = 0)$. Hence they contribute nothing to β, and, once they have been quantized, this paper will ignore them: but they will reappear in B.VI, because they do contribute to the mean-square vacuum fields.

The mode functions are chosen and normed for convenience. The (free) odd-parity amplitudes are

$$\left(\mathbf{E}^{\mathrm{TE},-}_{\mathbf{k},p}, \mathbf{B}^{\mathrm{TE},-}_{\mathbf{k},p}, \mathbf{E}^{\mathrm{TM},-}_{\mathbf{k},p}, \mathbf{B}^{\mathrm{TM},-}_{\mathbf{k},p}\right) = \exp(-\mathrm{i}\omega t + \mathrm{i}\mathbf{k}\cdot\mathbf{s}) \times \begin{pmatrix} \mathrm{i}(\hat{\mathbf{k}}\times\hat{\mathbf{z}})k\sin(pz) \\ (ck/\omega)\{-\mathrm{i}\hat{\mathbf{z}}k\sin(pz) + \hat{\mathbf{k}}p\cos(pz)\} \\ (ck/\omega)\{-\mathrm{i}\hat{\mathbf{z}}k\cos(pz) - \hat{\mathbf{k}}p\sin(pz)\} \\ -\mathrm{i}(\hat{\mathbf{k}}\times\hat{\mathbf{z}})k\cos(pz) \end{pmatrix}, \qquad (z > 0). \tag{2.17}$$

[5] Between two parallel sheets the situation may be different, because $p = 0$ might not then force the fields to vanish everywhere. Such differences may relate to the distinction that Robaschik and Wieczorek (1994) draw between matching conditions for what they call thick and thin reflectors.

The (interacting) even-parity modes subdivide into continuum (photon) modes, of both polarizations, and into bound modes (surface plasmons), which are purely TM. It may be worth stressing (i) that the surface plasmons are truly bound, i.e. they can travel parallel to the surface but cannot decay into or be excited by (are orthogonal to) photons; and (ii) that they are unique to flat geometries. For instance, on the spherical shell considered in B.III, they feature as narrow resonances in the scattering of TM photons with high angular momenta. Appendix A discusses how the surface modes show up in enumerating the degrees of freedom of the system.

The photon amplitudes are

$$\left(\mathbf{E}^{\mathrm{TE},+}_{\mathbf{k},p}, \mathbf{B}^{\mathrm{TE},+}_{\mathbf{k},p}, \mathbf{E}^{\mathrm{TM},+}_{\mathbf{k},p}, \mathbf{B}^{\mathrm{TM},+}_{\mathbf{k},p}\right) = \exp(-\mathrm{i}\omega t + \mathrm{i}\mathbf{k}\cdot\mathbf{s}) \times \begin{pmatrix} \mathrm{i}(\hat{\mathbf{k}}\times\hat{\mathbf{z}})k\cos(pz+\eta) \\ (ck/\omega)\{-\mathrm{i}\hat{\mathbf{z}}k\cos(pz+\eta) - \hat{\mathbf{k}}p\sin(pz+\eta)\} \\ (ck/\omega)\{\mathrm{i}\hat{\mathbf{z}}k\sin(pz+\mu) - \hat{\mathbf{k}}p\cos(pz+\mu)\} \\ \mathrm{i}(\hat{\mathbf{k}}\times\hat{\mathbf{z}})k\sin(pz+\mu) \end{pmatrix}, \qquad (z>0). \tag{2.18}$$

The bound-mode frequency[6] Ω, and a useful allied parameter $\tilde{p}$, are given by

$$(\Omega/c)^2 = \tfrac{1}{2}\left\{-q^2 + \sqrt{4q^2k^2+q^4}\right\} \equiv k^2 - \tilde{p}^2 = q\tilde{p}, \tag{2.19}$$

$$k^2 + \tilde{p}^2 = 2\tilde{p}(\tilde{p}+q/2), \qquad \mathrm{d}k\,k = \mathrm{d}\tilde{p}(\tilde{p}+q/2). \tag{2.20}$$

Conversely,

$$k_{\mathrm{sp}}^2 = (\Omega/cq)^2\{(\Omega/c)^2 + q^2\}.$$

Note the asymptotics[7]

$$\Omega(k \gg q) \simeq c\sqrt{qk} = \sqrt{2\pi n e^2 k/m} \equiv \Omega_{\mathrm{NR}}, \tag{2.21}$$

where Ω_{NR} is the surface-plasmon frequency in the NR model (appendix B); while, by contrast,

$$\Omega(k \ll q) \simeq ck. \tag{2.22}$$

Considering $\mathcal{R}^{\mathrm{TM}}$, $\mathcal{T}^{\mathrm{TM}}$ and $S^{\mathrm{TM}} = \exp(2\mathrm{i}\mu) = (1+\mathrm{i}\tan\mu)/(1-\mathrm{i}\tan\mu)$ as functions of p (or of ω) at fixed k, we can now see that they have the expected bound-state pole at $p = \mathrm{i}\tilde{p}$ (or at $\omega = \Omega$). In B.VI these poles prove important for calculating the mean-squared fields.

The amplitudes are

$$\begin{pmatrix}\mathbf{E}_{\mathbf{k}} \\ \mathbf{B}_{\mathbf{k}}\end{pmatrix} = \exp(-\mathrm{i}\Omega t + \mathrm{i}\mathbf{k}\cdot\mathbf{s} - \tilde{p}z) \begin{pmatrix} (ck/\Omega)(\hat{\mathbf{z}}k - \mathrm{i}\hat{\mathbf{k}}\tilde{p}) \\ \mathrm{i}(\hat{\mathbf{k}}\times\hat{\mathbf{z}})k \end{pmatrix}, \qquad (z>0). \tag{2.23}$$

If needed, fields and amplitudes at $z<0$ are determined by their parity:

$$E_{\parallel}^{\pm}(-z) = \pm E_{\parallel}^{\pm}(z), \qquad E_z^{\pm}(-z) = \mp E_z^{\pm}(z); \tag{2.24}$$

$$B_{\parallel}^{\pm}(-z) = \mp B_{\parallel}^{\pm}(z), \qquad B_z^{\pm}(-z) = \pm B_z^{\pm}(z). \tag{2.25}$$

[6] The dispersion relation (2.19) may be compared with equation (110) found by Fetter (1973) for a 2D Fermi gas: $\omega^2 = s^2k^2 + s^2k_{\mathrm{TF}}(k^2 - \omega^2/c^2)^{1/2}$. On the right we first use his (54) and (57b) to set $s^2 \equiv m^{-1}\partial p/\partial n = v_F^2/2$, where s is a sound velocity governed by the hydrodynamic pressure p, and v_F is the Fermi velocity; and then his (69a) to set $s^2k_{\mathrm{TF}} = qc^2$, where k_{TF} is the Thomas–Fermi screening constant, and q is our (2.5). Dividing through by c^2 and neglecting v_F^2/c^2 conformably with our disregard of pressure (or equivalently of any ground-state motion in the fluid if it were neutral), one obtains $(\omega/c)^2 = q\sqrt{k^2 - (\omega/c)^2}$, whose solution $\omega = \Omega$ reproduces (2.19).

[7] They may be compared with the surface-mode frequency ω_s on a 3D half-space with dielectric response $\varepsilon = 1 - \omega_p^2/\omega^2$. Then $\omega_s^2 = \omega_p^2/2 + c^2k^2 - (\omega_p^4/4 + c^4k^4)^{1/2}$ entails $\omega_s(k \gg \omega_p/c) \simeq \omega_p/\sqrt{2}$, quite unlike (2.21), while $\omega_s(k \ll \omega_p/c) \simeq ck$ just as in (2.22).

2.3. Quantization

The total energy (not yet a Hamiltonian) is

$$\int \mathrm{d}^2 s \frac{1}{2} nm\dot{\boldsymbol{\xi}}^2 + \int \mathrm{d}^2 s \int \mathrm{d}z \frac{1}{8\pi}(\mathbf{E}^2 + \mathbf{B}^2). \tag{2.26}$$

We must turn it into the quantal Hamiltonian

$$H = \frac{\hbar}{2}\int \mathrm{d}^2 k \int_0^\infty \mathrm{d}p \sum_j \omega\{a^{(j)\dagger}_{\mathbf{k},p} a^{(j)}_{\mathbf{k},p} + a^{(j)}_{\mathbf{k},p} a^{(j)\dagger}_{\mathbf{k},p}\} + \frac{\hbar}{2}\int \mathrm{d}^2 k \Omega\{a^\dagger_{\mathbf{k}} a_{\mathbf{k}} + a_{\mathbf{k}} a^\dagger_{\mathbf{k}}\}, \tag{2.27}$$

where j runs over the four combinations (TE, $\pm$) and (TM$\pm$), and

$$\left[a^{(j)}_{\mathbf{k},p}, a^{(j')\dagger}_{\mathbf{k}',p'}\right] = \delta_{jj'}\delta(\mathbf{k}-\mathbf{k}')\delta(p-p'), \qquad \left[a_{\mathbf{k}}, a^\dagger_{\mathbf{k}'}\right] = \delta(\mathbf{k}-\mathbf{k}'). \tag{2.28}$$

This is accomplished by writing the field operators, denoted generically by $\mathbf{F}^{(j)}$, as

$$\mathbf{F}^{(j)} = \int \mathrm{d}^2 k \int_0^\infty \mathrm{d}p \sqrt{\frac{\hbar\omega}{2\pi^2 k^2}} a^{(j)}_{\mathbf{k},p}\mathbf{F}^{(j)}_{\mathbf{k},p} + \int \mathrm{d}^2 k\, N_k a_{\mathbf{k}}\mathbf{F}_{\mathbf{k}} + Hc, \tag{2.29}$$

where Hc stands for the Hermitian conjugate, and the surface-plasmon normalization constant is given by

$$N_k^2 = \frac{\hbar\Omega^5}{2\pi c^4 q}\frac{1}{k^2(k^2+\tilde{p}^2)} = \frac{\hbar c}{2\pi}\frac{(q\tilde{p})^{3/2}}{k^2(2\tilde{p}+q)}. \tag{2.30}$$

The present paper aims to use (2.27)–(2.30) to determine, by summing over all normal modes, first the total-zero point energy β, and then the ground-state expectation value

$$\kappa \equiv \left\langle \int \mathrm{d}^2 s \frac{1}{2} nm\dot{\boldsymbol{\xi}}^2 \right\rangle \tag{2.31}$$

of the total kinetic energy, both per unit area. The latter will be needed to implement the restrictions to nonrelativistic motions of the fluid; besides, it is interesting in its own right because it shows how the retarded results depart from the virial theorem $\kappa = \beta/2$ which applies in the NR limit.

3. The zero-point cohesive energy β

3.1. Preliminaries

As explained in B.III, one obtains β by (i) subtracting, from the total zero-point energy per unit area of all modes, the corresponding sum in the absence of the mirror; and then (ii) further subtracting the self-energy of the same amount of fluid at infinite dilution. This self-energy is just the first Born approximation to the difference in (i), and for brevity we shall call the process *a Born subtraction*. It has certain formal similarities with a procedure central to the renormalizable theory devised by Graham and others (see, e.g., Graham *et al* (2004)), although the physics of their model is significantly different from ours. The two theories are compared in appendix D of B.III. Here we repeat only that in our model, which unlike theirs is dispersive but not covariant, the difference (ii) is finite for photon modes integrated over all p, i.e. over all photon frequencies ω realizable for given $\mathbf{k}$; but that the subsequent integration over $\mathbf{k}$ would diverge without the physically motivated Debye cutoff K.

The main albeit well-understood artificiality of our model, apologies for which will not be repeated, is that, like all purely plasma models, it makes β positive for all reasonable values of X. Even for a Fermi gas instead of a continuous fluid, truly cohesive energies, i.e. negative

β, would emerge only on taking into account the interactions between the ions that make up the true neutralizing background (see, e.g., Ashcroft and Mermin (1976)).

We subdivide

$$\beta = \beta_{\rm sp} + \beta_{\rm ph}, \tag{3.1}$$

where the subscripts sp and ph specify **s**urface-plasmons and photons.

It is of the essence that for β one needs only the spectrum, i.e. only the surface-mode dispersion relation (2.19) and the photon phase shifts (2.16); other details of the normal-mode amplitudes are irrelevant.

3.2. Surface plasmons

This is by far the simplest contribution, because it is not subject to subtractions of either kind. By hindsight we change the integration variable from k to $y = k/q$, with the upper limit $K/q = X$; define an auxiliary parameter

$$X_1 \equiv \tilde{p}(k = K)/q = \left[-1 + \sqrt{4X^2 + 1}\right]/2; \tag{3.2}$$

and find

$$\beta_{\rm sp} = \frac{1}{(2\pi)^2}\int_0^K 2\pi\, {\rm d}k k \frac{\hbar\Omega}{2} = \frac{\hbar c q^3}{4\pi^2}\mathcal{L}_{\rm sp}(X), \tag{3.3}$$

$$\mathcal{L}_{\rm sp}(X) \equiv \frac{\pi}{\sqrt{2}}\int_0^X {\rm d}y\, y\sqrt{-1 + \sqrt{4y^2+1}} = \frac{2\pi}{5}X_1^{5/2} + \frac{\pi}{3}X_1^{3/2}. \tag{3.4}$$

For realistically large X, evidently X_1 and X differ little. Then one has

$$\mathcal{L}_{\rm sp}(X) = X^{5/2}\pi\left\{\tfrac{2}{5} - \tfrac{1}{6}X^{-1} + \tfrac{1}{16}X^{-2} + \mathcal{O}(X^{-3})\right\}. \tag{3.5}$$

Since $X^{5/2} = (K/q)^{5/2}$, we can write

$$\beta_{\rm sp} = \frac{\hbar c q^3}{4\pi^2}\left\{\frac{2\pi}{5}X_1^{5/2} + \frac{\pi}{3}X_1^{3/2}\right\} = \frac{\hbar c\sqrt{q}K^{5/2}}{4\pi}\left\{\frac{2}{5} - \frac{1}{6}X^{-1} + \frac{1}{16}X^{-2} + \mathcal{O}(X^{-3})\right\}. \tag{3.6}$$

The leading term is just the nonretarded result $\beta_{\rm NR}$, while the others represent retardation corrections that vanish as $X \to \infty$.

By contrast, the (unrealistic) perfect-reflector limit would entail $X \to 0$, whence

$$X_1 \simeq X^2 \quad \Rightarrow \quad \beta_{\rm sp} \simeq \hbar c q^3 X^3/12\pi = \hbar c K^3/12\pi \qquad (\text{as } X \to 0). \tag{3.7}$$

3.3. Photons

3.3.1. The general theory. We deal separately with the two polarizations:

$$\beta_{\rm ph} = \beta_{\rm TE} + \beta_{\rm TM}. \tag{3.8}$$

For brevity we omit the subscripts whenever the context prevents ambiguity, and use δ generically for the phase shifts η or μ.

To determine the β we adapt the strategy of B.III as follows. (i) Discretize p by imposing the auxiliary boundary conditions that $\mathbf{E}_\parallel$ vanish at $z = \pm L$; (ii) determine, for given $\mathbf{k}$, by how much the allowed values p_n are changed on account of the phase shifts, and the corresponding changes in the allowed frequencies $\omega_n \equiv c\sqrt{p_n^2 + k^2}$; (iii) find the sum, call it $Z(\mathbf{k})$, of the consequent *changes* in ZPE for given $\mathbf{k}$ as $L \to \infty$, converting $\sum_n$ into $\int {\rm d}p$ in (almost) standard fashion; (iv) obtain the integral γ of $Z(\mathbf{k})$ over all $\mathbf{k}$ admitted by the Debye cutoff $k < K$; and finally (v) obtain β by subtracting from γ the appropriate Born counter-term.

Since only modes with even $\mathbf{E}_\parallel$ contribute, we need consider only $z > 0$, where $\mathbf{E}_\parallel$ for either polarization varies as $\cos[p_n z + \delta(p_n)]$. Recall that, to avoid redundancy, p and the p_n are defined to be non-negative. In fact the p_n must be strictly positive: they cannot be zero, because then $\mathbf{E}_\parallel$ would be a constant, and would vanish everywhere if it vanished at $z = L$.

The boundary conditions impose

$$\cos[p_n L + \delta(p_n)] = 0 \quad \Rightarrow \quad p_n L + \delta(p_n) = (n + 1/2)\pi, \tag{3.9}$$

with non-negative integer

$$n = n(\min), (n(\min) + 1), (n(\min) + 2), \ldots .$$

Without the sheet, indicated by superscript (0), we have $\delta = 0$, whence (3.9) and $p_n > 0$ entail

$$p_n^{(0)} = (n + 1/2)\pi/L, \qquad n^{(0)}(\min) = 0, \qquad p^{(0)}(\min) = \pi/2L.$$

For TE modes with the sheet, $\eta(0) = -\pi/2$, whence

$$p_n^{(\mathrm{TE})} = (n + 1)\pi/L, \qquad n^{(\mathrm{TE})}(\min) = 0, \qquad p^{(\mathrm{TE})}(\min) = \pi/L.$$

For TM modes with the sheet, $\mu(p = 0, k \neq 0) = 0$, the same as without the sheet, whence the consequences are also the same: $\left[p_n^{(\mathrm{TM})}, n^{(\mathrm{TM})}(\min), p_n^{(\mathrm{TM})}\right] = \left[p_n^{(0)}, n^{(0)}(\min), p_n^{(0)}\right]$. The upshot is that with or without the sheet, and for both polarizations, $n(\min) = 0$.

At very high n and thereby very high p, modes with and without the sheet correspond one to one, because the $\delta(p_n)$ vanish. Thus the shift Δp_n and the resultant frequency shift $\Delta\omega_n$ induced by the sheet are

$$\Delta p_n = -\delta(p_n, k)/L, \qquad \Delta\omega_n(k) = -\frac{c^2 p}{\omega L}\delta(p_n, k), \tag{3.10}$$

and the Euler–Maclaurin formula yields the precise version of the rule usually quoted in the somewhat loose form that $\sum_n \to \int \mathrm{d}n \to (L/\pi)\int \mathrm{d}p$, namely

$$\sum_{n=0}^{\infty} \frac{\hbar}{2}\Delta\omega_n = \frac{\hbar}{2}\Delta\omega_0/2 + \frac{L}{\pi}\int_{p(\min)}^{\infty} \mathrm{d}p \frac{\hbar}{2}\Delta\omega(p, k) + \cdots, \tag{3.11}$$

up to terms that vanish as $L \to \infty$. *The sum and the integrals in (3.11)–(3.13) diverge: they must be understood as short-hand place-holders for the well-defined expressions $\mathcal{L}_{\mathrm{TE,TM}}$ that emerge once the Born counterterms are subtracted explicitly in (3.15) and (3.16).*

Fortunately we can simplify (3.11) by observing that the lower limit, the integrand and the addend $\Delta\omega_{n(\min)}/2$ are all of order $1/L$; therefore, as $L \to \infty$ we can drop the addend, and replace the lower limit[8] by 0. Then γ follows on integrating over all admissible $\mathbf{k}$ (which means acting with $\int \mathrm{d}^2k \big/ \big((2\pi)^2 = 1/(2\pi)\int_0^K \mathrm{d}k\, k\big)$:

$$\gamma = -\frac{\hbar}{4\pi^2}\int_0^K \mathrm{d}k\, k \int_0^\infty \mathrm{d}p \frac{c^2 p}{\omega}\delta. \tag{3.12}$$

In terms of conveniently scaled integration variables this becomes

$$\gamma = -\frac{\hbar c q^3}{4\pi^2}\int_0^X \mathrm{d}y\, y \int_0^\infty \mathrm{d}x \frac{x}{\sqrt{x^2 + y^2}}\delta, \qquad y \equiv k/q, \quad x \equiv p/q, \quad X \equiv K/q. \tag{3.13}$$

It remains to identify the counterterms. By construction, γ already excludes the ZPE of the pertinent photons (those with $k < K$) in the absence of the sheet. What we need to subtract is the self-energy of a mass nm of fluid at infinite dilution, given by that part of γ

[8] Thus the precise value of $n(\min)$ turns out to be irrelevant to β. It matters only if one requires (as in Levinson's theorem, appendix A) the total *number* rather than the total *energy* of the photon modes.

that is proportional to n as $n \to 0$. Because each $\tan\delta$ already has an explicit factor of q, and thereby of n, one obtains the counterterm by replacing the phase-shifts by the first Born approximation, i.e. by replacing the arctangents by their argument. Thus we find

$$\beta_{\mathrm{TE,TM}} = \frac{\hbar c q^3}{4\pi^2}\mathcal{L}_{\mathrm{TE,TM}}, \tag{3.14}$$

featuring the convergent integrals

$$\mathcal{L}_{\mathrm{TE}} = \int_0^X \mathrm{d}y\, y \int_0^\infty \mathrm{d}x \frac{x}{\sqrt{x^2+y^2}} \left\{ \tan^{-1}\left(\frac{1}{x}\right) - \frac{1}{x} \right\}, \tag{3.15}$$

$$\mathcal{L}_{\mathrm{TM}} = \int_0^X \mathrm{d}y\, y \int_0^\infty \mathrm{d}x \frac{x}{\sqrt{x^2+y^2}} \left\{ \tan^{-1}\left(\frac{x}{x^2+y^2}\right) - \frac{x}{x^2+y^2} \right\}. \tag{3.16}$$

Since $\tan^{-1}(z) < z$, both $\beta_{\mathrm{TE,TM}}$ are negative.

In view of this pattern we write

$$\mathcal{L}_{\mathrm{TE,TM}} = \int_0^X \mathrm{d}y\, y\mathcal{H}_{\mathrm{TE,TM}}(y), \tag{3.17}$$

where $\mathcal{H}_{\mathrm{TE,TM}}$ stand for the integrals over x in (3.15), (3.16).

Finally, it should be mentioned for completeness that the contribution to the zero-point energy from the modes of the continuous spectrum can be approached in another way, namely through the change in ρ, their density of states. The other method starts from (3.9), increments n by $\mathrm{d}n = 1$, and observes that the corresponding increment of p is given by $\mathrm{d}p(L + \partial\delta/\partial p) = \pi\,\mathrm{d}n$. In the continuum limit $L \to \infty$ this yields

$$\sum_n \cdots \to \int \mathrm{d}n \cdots = (1/\pi) \int \mathrm{d}p(L + \partial\delta/\partial p) \ldots,$$

between integration limits that deserve attention, for reasons to be mentioned presently. The L-proportional component is precisely what one has in the absence of the sheet, whence it is dropped; the term with the derivative of the phase shift can be viewed as a change that the sheet forces on ρ, with a consequent change $(1/2\pi)\int \mathrm{d}p(\partial\delta/\partial p)\omega(k, p)$ of zero-point energy. If the channel in question has bound modes, their contributions must be added by hand; and each method requires some care to identify and subtract the self-energy consistently. The method used here is the same as in B.III, its consistency in these respects largely checked by the NR limit, where there are no such complications. Which method one adopts is a matter of taste: we have chosen to start directly from the shifts $\Delta\omega_n$, partly because they seem closer to first principles, and partly because integrands featuring the δ rather than the $\partial\delta/\partial p$ are somewhat easier to handle.

However, one should note that some caution is needed to go directly from the formulae of either method to those of the other: complete security with the integrations by parts connecting $\int \mathrm{d}p(\partial\delta/\partial p)\omega$ and $\int \mathrm{d}p(\partial\omega/\partial p)\delta$ requires a grip on the threshold behaviour of the phase shifts, i.e. on Levinson's theorem from appendix A, and therefore also on the role of the bound modes. The Casimir effect with finite-mass photons (Barton and Dombey 1985) affords an even more telling example of the need for such caution. By contrast, for simpler problems without bound modes it is often the density-of-state methods that are preferable: as for instance for a 1D analogue of our present model (Barton and Calogeracos 1995).

3.3.2. Results. By contrast to most calculations in B.VI, it is easiest to determine $\mathcal{H}_{\mathrm{TE,TM}}$ by integrating along the real x-axis: one reason is that the counterterm (i.e. the second term) in $\mathcal{L}_{\mathrm{TM}}$ as it stands is not integrable at the branch point $x = \mathrm{i}y$. All the integrals can be found in closed form[9]. They (especially $\mathcal{H}_{\mathrm{TM}}$) consume more time than any other evaluation in this paper, and the critical steps are sketched in appendix C. Fortunately, the subsequent integrations over y are comparatively straightforward.

It proves convenient to introduce the parameters

$$X_1 \equiv \tfrac{1}{2}\big[\sqrt{4X^2+1}-1\big], \qquad X_2 \equiv \tfrac{1}{2}\big[\sqrt{4X^2+1}+1\big], \qquad X_3 \equiv \sqrt{X^2-1}, \tag{3.18}$$

with X_1 as in (3.2), and with $X_{1,2}$ satisfying the identities

$$X_2 - X_1 = 1, \qquad X_1 X_2 = X^2, \qquad X^2 - X_1^2 = X_1, \qquad X_2^2 - X^2 = X_2. \tag{3.19}$$

For very large and for very small X

$$X_{1,2} = X \mp 1/2 + \mathcal{O}(1/X), \qquad X_3 = X + \mathcal{O}(1/X), \tag{3.20}$$

$$X_1 = X^2 + \mathcal{O}(X^4), \qquad X_2 = 1 + X^2 + \mathcal{O}(X^4). \tag{3.21}$$

For the TE modes appendix C obtains

$$\mathcal{H}_{\mathrm{TE}} = 1 - \frac{\pi y}{2} + \begin{pmatrix} -\sqrt{1-y^2}\tanh^{-1}(\sqrt{1-y^2}), & (y<1) \\ \sqrt{y^2-1}\tan^{-1}(\sqrt{y^2-1}), & (y>1) \end{pmatrix}. \tag{3.22}$$

Accordingly, to integrate over y one needs to distinguish between the case[10] $X < 1$, which requires only the first line of (3.22), and the case $X > 1$, which requires both lines. Changing the integration variable from y to y^2 one finds

$$\mathcal{L}_{\mathrm{TE}} = \frac{1}{3}X^2 - \frac{\pi}{6}X^3 + \frac{1}{3}\log\left(\frac{X}{2}\right) + \frac{1}{3}\begin{pmatrix} |X_3|^3\tanh^{-1}(|X_3|), & (X<1) \\ X_3^3\tan^{-1}(X_3), & (X>1) \end{pmatrix}. \tag{3.23}$$

Note that the upper and lower entries have opposite signs in (3.22), but the same sign in (3.23).

For the TM modes, appendix C eventually finds

$$\mathcal{L}_{\mathrm{TM}} = \frac{4X^2}{5} - \frac{1}{15}\log\left(\frac{X}{2}\right) - \left[\frac{2X_1^{5/2}}{5} + \frac{X_1^{3/2}}{3}\right]\tan^{-1}\left(\frac{1}{\sqrt{X_1}}\right) - \left[\frac{2X_2^{5/2}}{5} - \frac{X_2^{3/2}}{3}\right]\tanh^{-1}\left(\frac{1}{\sqrt{X_2}}\right). \tag{3.24}$$

3.4. General patterns and asymptotics

The photon contributions $\beta_{\mathrm{TE,TM}}$, which are negative, may now be compared with the surface-plasmon contribution β_{sp} from section 3.2, which is positive. Conformably to (3.1) and (3.8) we define

$$\mathcal{L}_{\mathrm{TE}} + \mathcal{L}_{\mathrm{TM}} = \mathcal{L}_{\mathrm{ph}}, \qquad \mathcal{L}_{\mathrm{ph}} + \mathcal{L}_{\mathrm{sp}} = \mathcal{L}. \tag{3.25}$$

[9] The writer has learnt the hard way that this is better done by hand than with MAPLE, which in some cases gives up, and in several others delivers expressions that take longer to reformulate intelligibly than to evaluate *ab initio* on paper.

[10] Here it proves better to use $\tanh^{-1}(z) = (1/2)\log[(1+z)/(1-z)]$. Hindsight shows that the end-results for $X \lessgtr 1$ are linked by analytic continuation, but there is so much scope for choosing wrong branches that it is unsafe to proceed except by independent calculations for the two cases. The same is true for $y \lessgtr 1$ in (3.22).

Interest attaches also to the total TM contribution

$$\mathcal{L}_{TM,\text{total}} = \mathcal{L}_{\text{sp}} + \mathcal{L}_{\text{TM}}, \qquad \mathcal{L}_{\text{TE}} + \mathcal{L}_{TM,\text{total}} = \mathcal{L}. \tag{3.26}$$

In the realistic scenario $X \gg 1$, the asymptotic expansions read

$$\mathcal{L}_{\text{TE}}(X \to \infty) = -\frac{\pi X}{4} + \frac{1}{3}\log\left(\frac{X}{2}\right) + \frac{4}{9} + \mathcal{O}\left(\frac{1}{X}\right), \tag{3.27}$$

$$\mathcal{L}_{\text{TM}}(X \to \infty) = -\frac{1}{15}\log\left(\frac{X}{2}\right) - \frac{31}{225} + \mathcal{O}(X^{-3/2}), \tag{3.28}$$

$$\mathcal{L}_{\text{sp}}(X \to \infty) = \frac{2\pi}{5}X^{5/2} - \frac{\pi}{6}X^{3/2} + \frac{\pi X^{1/2}}{16} + \mathcal{O}(X^{-1/2}). \tag{3.29}$$

Thus TE dominate TM photons, but surface plasmons dominate both. Therefore the end-result is positive; in fact it is practically the same as for the NR model: recall from (2.6) that $\hbar c q^3 X^{5/2}$ is free of c.

In the fanciful scenario $X \ll 1$, where X is no longer estimated as on the right of (2.5), one has

$$\mathcal{L}_{\text{TE}}(X \to 0) = X^2\left[\frac{1}{2}\log\left(\frac{X}{2}\right) + \frac{1}{4}\right] - X^3\left[\frac{\pi}{6}\right] + X^4\left[-\frac{1}{8}\log\left(\frac{X}{2}\right) + \frac{3}{32}\right] + \mathcal{O}(X^5), \tag{3.30}$$

$$\mathcal{L}_{\text{TM}}(X \to 0) = X^2\left[\frac{1}{2}\log\left(\frac{X}{2}\right) + \frac{3}{4}\right] - X^3\left[\frac{\pi}{6}\right] + X^4\left[\frac{1}{8}\log\left(\frac{X}{2}\right) + \frac{1}{32}\right] + \mathcal{O}(X^5), \tag{3.31}$$

$$\mathcal{L}_{\text{sp}}(X \to 0) = \frac{\pi X^3}{3} - \frac{\pi X^5}{10} + \mathcal{O}(X^7). \tag{3.32}$$

Thus TE and TM photons contribute comparably, and dominate surface plasmons. Therefore the end-result is negative.

Between the asymptotic regions the various $\mathcal{L}$ must be evaluated numerically: all sign changes occur below but close to $X = 1$. Figure 1 shows the (negative) photon contributions, $\mathcal{L}_{\text{TE}}$ and $\mathcal{L}_{\text{TM}}$; figure 2 compares $\mathcal{L}_{\text{ph}} \equiv \mathcal{L}_{\text{TE}} + \mathcal{L}_{\text{TM}}$, the (positive) surface-plasmon contribution $\mathcal{L}_{\text{sp}}$, and their sum $\mathcal{L}$, which has a zero near $X = 0.7$. Figure 3 concerns only the TM sector, comparing the negative photon contribution $\mathcal{L}_{\text{TM}}$, the positive surface-plasmon contribution $\mathcal{L}_{\text{sp}}$, and their sum $\mathcal{L}_{\text{TM,total}}$, which changes sign near $X = 0.33$. Figure 4 shows the alternative decomposition of $\mathcal{L}_{\text{sp}}$ (already featured in figure 2) into its TE and its total TM components.

Finally we record β itself, to leading order:

$$\beta(K/q \gg 1) \simeq \frac{\hbar c q^3}{4\pi^2}\frac{2\pi}{5}\left(\frac{K}{q}\right)^{5/2} = \frac{\hbar c q^{1/2} K^{5/2}}{10\pi}, \tag{3.33}$$

$$\beta(K/q \ll 1) \simeq -\frac{\hbar c q^3}{4\pi^2}\left(\frac{K}{q}\right)^2\left[\log\left(\frac{2q}{K}\right) - \frac{1}{2}\right] = -\frac{\hbar c q K^2}{4\pi^2}\left[\log\left(\frac{2q}{K}\right) - \frac{1}{2}\right]. \tag{3.34}$$

Notice from (3.34) that β diverges as $q \to \infty$, i.e. in the PR limit: *contrary to folklore, the surface energy of perfect reflectors is negative infinite rather than zero*.

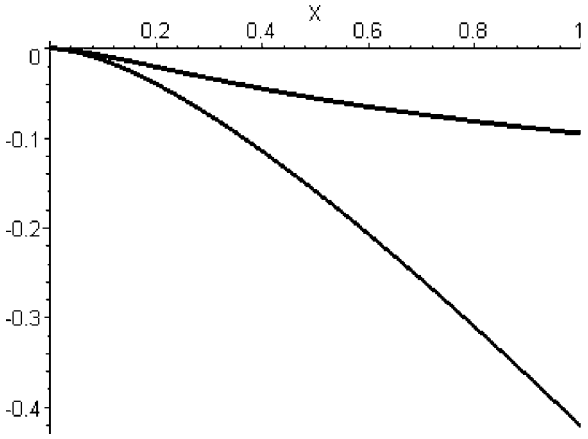

Figure 1. The components of $\mathcal{L}_{\rm ph} \equiv \mathcal{L}_{\rm TE} + \mathcal{L}_{\rm TM}$. Top curve: $\mathcal{L}_{\rm TM}$; bottom curve: $\mathcal{L}_{\rm TE}$.

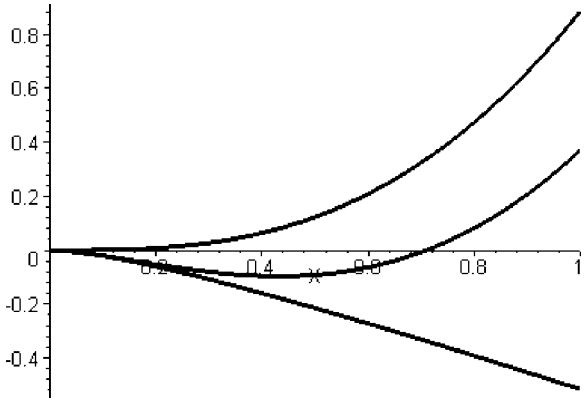

Figure 2. The surface-plasmon and photon contributions to $\mathcal{L} \equiv \mathcal{L}_{\rm sp} + \mathcal{L}_{\rm ph}$. The top, middle and bottom curves show $\mathcal{L}_{\rm sp}$, $\mathcal{L}$ and $\mathcal{L}_{\rm ph}$, respectively.

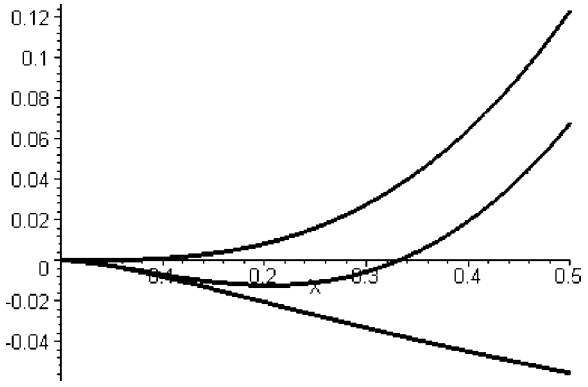

Figure 3. The surface-plasmon and photon parts of the transverse-magnetic sector. The top, bottom and middle curves show $\mathcal{L}_{\rm sp}$, $\mathcal{L}_{\rm TM}$ and $\mathcal{L}_{\rm TM,total} \equiv \mathcal{L}_{\rm sp} + \mathcal{L}_{\rm TM}$, respectively. The horizontal scale is twice that in figures 1, 2 and 4.

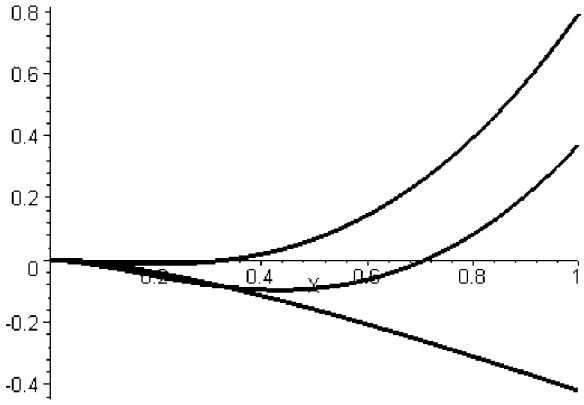

Figure 4. The TE and the total TM contributions to $\mathcal{L} \equiv \mathcal{L}_{\rm TE} + \mathcal{L}_{\rm TM,total}$. The top, middle and bottom curves show $\mathcal{L}_{\rm TM,total}$, $\mathcal{L}$ and $\mathcal{L}_{\rm TE}$, respectively. The zero of $\mathcal{L}_{\rm TM,total}$ evident in figure 3 is barely visible, because of the smaller vertical scale.

3.5. Boyer terms

We digress briefly to look for analogues of what in B.III were called *Boyer terms*, defined as components of the energy that are independent of the material constants parametrizing the response function. As already mentioned, for the *total* cohesive energies of spheres of radius R, dimensionalities admit such components proportional to $\hbar c/R$; indeed, it is from their study by Boyer (1968) that our field of enquiry has grown. By contrast, for an energy *per unit area,* the absence of geometric parameters like R means that components of β can be free of material constants either (i) in the sense of being free of q, or (ii) in the sense of being free of the cutoff K and thereby of X , but that they cannot be free of both.

A dimensional check identifies Boyer terms of type (i) as components of $\mathcal{L}$ proportional to X^3. Equations (3.27)–(3.29) show that for $X \gg 1$ there are none. For $X \ll 1$, we see from (3.30)–(3.32) that such terms do occur as subdominant parts of $\mathcal{L}_{\rm TE}$ and $\mathcal{L}_{\rm TM}$, and as the dominant part of $\mathcal{L}_{\rm sp}$; but by a remarkable coincidence they cancel from the end-result $\mathcal{L}$. Consequently, the expansion of $\mathcal{L}$ jumps from order X^2 to order X^4:

$$\mathcal{L} = X^2\left[\log\left(\frac{X}{2}\right) + \frac{1}{2}\right] + X^4\left[\frac{1}{8}\right] + \mathcal{O}(X^5), \tag{3.35}$$

whose leading term yields (3.34).

By contrast, Boyer terms of type (ii) are visible in (3.27) and (3.28): their (again subdominant) contribution to $\mathcal{L}_{\rm ph}$ and thence to $\mathcal{L}$ is $(4/9 - 31/225) = 23/75$.

4. The mean kinetic energy κ

4.1. Preliminaries

We determine κ, the ground-state expectation value per unit area of the kinetic energy of the fluid. It is interesting because (i) it shows just how the exact results depart from the requirement $\kappa_{\rm NR} = \beta_{\rm NR}/2$ of the nonrelativistic virial theorem for the nonretarded model (appendix B); (ii) it identifies, by default, the part $(\beta - \kappa)$ of the cohesive energy that resides in the fields, i.e. off the sheet; and (iii) it is needed to check for contraventions of our basic assumption that the fluid moves nonrelativistically (section 4.3).

For comparison with β and $\mathcal{L}$, we define

$$\kappa \equiv \frac{\hbar c q^3}{4\pi^2}\mathcal{K}(X), \qquad \mathcal{K} = \mathcal{K}_{\rm ph} + \mathcal{K}_{\rm sp}, \qquad \mathcal{K}_{\rm ph} = \mathcal{K}_{\rm TE} + \mathcal{K}_{\rm TM}. \tag{4.1}$$

The chief novelty is that, to determine κ (unlike β), one must have quantized the system explicitly, as in sections 2.2 and 2.3, because now one needs the relation between the fluid velocity and $\mathbf{E}_\parallel(z=0)$. This stems from (2.8), and for *each normal mode* reads

$$\dot{\boldsymbol{\xi}} = (\mathrm{i}e/m\omega)\mathbf{E}_\parallel(z=0), \tag{4.2}$$

where ω is Ω for surface plasmons, and $c(k^2+p^2)^{1/2}$ for photons.

For surface plasmons, the mode expansion (2.29) with the amplitude (2.23) yields

$$\kappa_{\rm sp} = \int \mathrm{d}^2k \frac{1}{2} nm \left(\frac{e}{m\Omega}\right)^2 N_k^2 \left(\frac{ck}{\Omega}\right)^2 \tilde{p}^2.$$

One uses (2.30) for N_k^2, eliminates Ω in favour of $\tilde{p}$ by (2.19), and changes the integration variable from k to $\tilde{p}$ by (2.20). This leads straightforwardly to

$$\mathcal{K}_{\rm sp} = \frac{\pi}{5} X_1^{5/2}, \tag{4.3}$$

with X_1 as in (3.2) and (3.18). Recalling that $X \gg 1$ entails $X_1 \simeq X$, we see that $\mathcal{K}_{\rm sp}$ then constitutes half the leading term of $\mathcal{L}_{\rm sp}$ as given by (3.6).

For photons,

$$\kappa_{\rm ph} = \sum_{j={\rm TE+,TM+}} \int_0^K 2\pi\, \mathrm{d}k\, k \int_0^\infty \mathrm{d}p \frac{1}{2} nm \langle \dot{\boldsymbol{\xi}}_{\mathbf{k},p}^{(j)2} \rangle. \tag{4.4}$$

We use the expansion (2.29) with the normal-mode amplitudes (2.18), the dimensionless integration variables from (3.13), and find

$$\mathcal{K}_{\rm TE} = \int_0^X \mathrm{d}y\, y \int_0^\infty \frac{\mathrm{d}x}{\sqrt{x^2+y^2}} \{\cos^2(\eta) - 1\} = -\int_0^X \mathrm{d}y\, y \int_0^\infty \frac{\mathrm{d}x}{\sqrt{x^2+y^2}} \frac{1}{[x^2+1]}, \tag{4.5}$$

$$\begin{aligned}\mathcal{K}_{\rm TM} &= \int_0^X \mathrm{d}y\, y \int_0^\infty \frac{\mathrm{d}x x^2}{(x^2+y^2)^{3/2}} \{\cos^2(\mu) - 1\} \\ &= -\int_0^X \mathrm{d}y\, y \int_0^\infty \frac{\mathrm{d}x}{(x^2+y^2)^{3/2}} \frac{x^4}{\left[(x^2+y^2)^2 + x^2\right]}.\end{aligned} \tag{4.6}$$

The -1 in the initial combinations $\{\cos^2(\delta) - 1\}$ are the Born subtractions, on exactly the same footing as in the parallel expressions for β. They subtract the kinetic energy induced in the fluid by the Maxwell field unaware of the sheet, i.e. with the phase shifts set equal to zero. Like $\mathcal{L}_{\rm TE,TM}$, both $\mathcal{K}_{\rm TE,TM}$ are evidently negative.

4.2. Results

For TE, equation (4.5) leads to

$$\mathcal{K}_{\rm TE} = -\int_0^X \mathrm{d}y\, y \left\{ \Theta(1-y) \frac{\tanh^{-1}(\sqrt{1-y^2})}{\sqrt{1-y^2}} + \Theta(y-1) \frac{\tan^{-1}(\sqrt{y^2-1})}{\sqrt{y^2-1}} \right\}, \tag{4.7}$$

where Θ is the Heaviside step-function; and thence to

$$\mathcal{K}_{\rm TE}(X) = \log\left(\frac{X}{2}\right) + \begin{pmatrix} |X_3| \tanh^{-1}(|X_3|), & (X<1) \\ -X_3 \tan^{-1}(X_3), & (X>1) \end{pmatrix}. \tag{4.8}$$

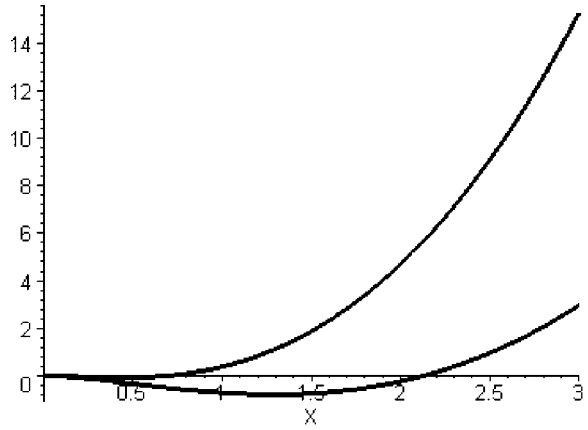

Figure 5. Comparing β with the mean kinetic energy κ. The top and bottom curves show their respective scaling factors $\mathcal{L}$ and $\mathcal{K}$. The zero of $\mathcal{L}$ evident in figures 2 and 4 is barely visible, because of the much smaller horizontal scale.

For TM, one must evaluate the x-integral in (4.6), one of the more painful calculations in this paper. Eventually one finds, with $x_{1,2} \equiv (\sqrt{4y^2+1} \mp 1)/2$ as in appendix C, that

$$\mathcal{K}_{\mathrm{TM}} = \int_0^X \mathrm{d}y\, y \left\{ 1 - \frac{1}{\sqrt{4y^2+1}} \left[x_1^{3/2} \tan^{-1}\left(\frac{1}{\sqrt{x_1}}\right) + x_2^{3/2} \tanh^{-1}\left(\frac{1}{\sqrt{x_2}}\right) \right] \right\}$$
$$= \frac{2}{5}X^2 - \frac{1}{5}\log\left(\frac{X}{2}\right) - \frac{X_1^{5/2}}{5}\tan^{-1}\left(\frac{1}{\sqrt{X_1}}\right) - \frac{X_2^{5/2}}{5}\tanh^{-1}\left(\frac{1}{\sqrt{X_2}}\right). \tag{4.9}$$

The asymptotics, to be compared with those of β, equations (3.27)–(3.32), read

$$\mathcal{K}_{\mathrm{TE}}(X \to \infty) = -\frac{\pi X}{2} + \log\left(\frac{X}{2}\right) + 1 + \mathcal{O}(X^{-1}), \tag{4.10}$$

$$\mathcal{K}_{\mathrm{TM}}(X \to \infty) = -\frac{1}{5}\log\left(\frac{X}{2}\right) - \frac{26}{75} + \mathcal{O}(X^{-3/2}), \tag{4.11}$$

$$\mathcal{K}_{\mathrm{sp}}(X \to \infty) = \frac{\pi X^{5/2}}{5} - \frac{\pi X^{3/2}}{4} + \frac{5\pi X^{1/2}}{32} + \mathcal{O}(X^{-1/2}); \tag{4.12}$$

$$\mathcal{K}_{\mathrm{TE}}(X \to 0) = X^2\left[\frac{1}{2}\log\left(\frac{X}{2}\right) - \frac{1}{4}\right] + X^4\left[\frac{1}{8}\log\left(\frac{X}{2}\right) + \frac{1}{32}\right] + \mathcal{O}(X^6), \tag{4.13}$$

$$\mathcal{K}_{\mathrm{TM}}(X \to 0) = X^2\left[\frac{1}{2}\log\left(\frac{X}{2}\right) + \frac{1}{4}\right] - X^4\left[\frac{1}{8}\log\left(\frac{X}{2}\right) + \frac{5}{32}\right] + \mathcal{O}(X^5), \tag{4.14}$$

$$\mathcal{K}_{\mathrm{sp}}(X \to 0) = \frac{\pi X^5}{5} - \frac{\pi X^7}{2} + \mathcal{O}(X^9). \tag{4.15}$$

The orders of magnitude and the qualitative pattern of the $\mathcal{K}$ are much the same as those of the analogous functions $\mathcal{L}$ for β. To make this clear, figure 5 plots the resultants $\mathcal{K}$ and $\mathcal{L}$, and tables 1 and 2 indicate the asymptotically leading terms of their constituents, along with their ratios. They show that the familiar virial theorem $\mathcal{K}/\mathcal{L} = 1/2$ never applies to photons, neither for large X nor for small; nor to surface plasmons at small X. But for large X it does apply, to leading order, to the surface plasmons, and thereby to $\mathcal{K}$ and $\mathcal{L}$ in toto: under these conditions roughly half of β is indeed potential energy, in the sense that it resides in the fields (on closer examination, in the electric field).

Table 1. Leading terms when $X \gg 1$.

	TE	TM	sp	Total
$\mathcal{L}$	$-X\left[\frac{\pi}{4}\right]$	$-\frac{1}{15}\log\left(\frac{X}{2}\right)-\frac{31}{225}$	$X^{5/2}\left[\frac{2\pi}{5}\right]$	$\simeq\mathcal{L}_{\rm sp}$
$\mathcal{K}$	$-X\left[\frac{\pi}{2}\right]$	$-\frac{1}{5}\log\left(\frac{X}{2}\right)-\frac{26}{75}$	$X^{5/2}\left[\frac{\pi}{5}\right]$	$\simeq\mathcal{K}_{\rm sp}$
$\mathcal{K}/\mathcal{L}$	2	$3+\mathcal{O}(1/\log(X)$	1/2	$\simeq 1/2$

Table 2. Leading terms when $X \ll 1$.

	TE	TM	sp	Total
$\mathcal{L}$	$X^2\left[\frac{1}{2}\log\left(\frac{X}{2}\right)+\frac{1}{4}\right]$	$X^2\left[\frac{1}{2}\log\left(\frac{X}{2}\right)+\frac{3}{4}\right]$	$X^3\left[\frac{\pi}{3}\right]$	$\simeq\mathcal{L}_{\rm ph}\simeq X^2\left[\log\left(\frac{X}{2}\right)+1\right]$
$\mathcal{K}$	$X^2\left[\frac{1}{2}\log\left(\frac{X}{2}\right)-\frac{1}{4}\right]$	$X^2\left[\frac{1}{2}\log\left(\frac{X}{2}\right)+\frac{1}{4}\right]$	$X^5\left[\frac{\pi}{5}\right]$	$\simeq\mathcal{K}_{\rm ph}\simeq X^2\log\left(\frac{X}{2}\right)$
$\mathcal{K}/\mathcal{L}$	$1+\mathcal{O}(1/\log(X)$	$1+\mathcal{O}(1/\log(X)$	$X^2\left[\frac{3}{5}\right]$	$\simeq\mathcal{K}_{\rm ph}/\mathcal{L}_{\rm ph}\simeq 1+\mathcal{O}(1/\log(X)$

4.3. The inconsistency of very strong coupling ($X \to 0$)

At this point one can show that *very* small X is incompatible with our underlying assumption that the fluid moves nonrelativistically. For that to be the case $|\kappa|$ must evidently be much less than the rest-energy nmc^2 per unit area, requiring $\chi \ll 1$, with the ratio χ defined as

$$\chi \equiv \left|\frac{\kappa}{nmc^2}\right| = \frac{1}{nmc^2}\frac{\hbar c q^3}{4\pi^2}\,|\mathcal{K}| = \frac{2}{\sqrt{\pi}}\left(\frac{(\lambda_c/2\pi)}{a}\right)\frac{1}{X^3}|\mathcal{K}(X)|, \qquad \lambda_c/2\pi \equiv \hbar/mc. \tag{4.16}$$

Evidently $\lambda_c/2\pi$ is the reduced Compton wavelength of the charge carriers; in reasonable models of nonrelativistic systems it should be much shorter than the mean spacing a, so that

$$\lambda_c/2\pi a \ll 1. \tag{4.17}$$

Note that this is a purely geometric condition, independent of the coupling-strength parameter q. More specifically, if we envisage the charge carriers as electrons, and correspondingly take $a \sim a_B$, then

$$\lambda_c/2\pi a \sim \alpha \simeq 1/137. \tag{4.18}$$

As $X \to \infty$, table 1 reminds one that $\mathcal{K} \sim X^{5/2}$, whence

$$\chi \sim (\lambda_c/2\pi a)\,X^{-1/2} \ll 1, \qquad (X \gg 1), \tag{4.19}$$

as required. With (4.18) and with the corresponding estimate $X \sim 1/\alpha^2$, one would have $\chi \sim \alpha^2 \sim 10^{-4}$, the typical relative order of magnitude of relativistic corrections in atomic physics.

By contrast, as $X \to 0$, table 2 gives $\mathcal{K} \sim X^2\log(X)$, whence

$$\chi \sim (\lambda_c/2\pi a)\,X^{-1}\log(X), \qquad (X \ll 1). \tag{4.20}$$

To appreciate the implications, we recall that only $X \sim a/r_0 = amc^2/e^2$ depends on the interaction between the plasma and the field. Thus the strong-coupling limit is best envisaged as $X \to 0$ at fixed $\lambda_c/2\pi a$, and it is in this sense that (disregarding the logarithm),

$$\chi \ll 1 \quad \Rightarrow \quad X \gg \lambda_c/2\pi a \sim \alpha \sim 10^{-2}, \qquad (X \ll 1), \tag{4.21}$$

if we adhere to estimate (4.18). Admittedly this condition is not all that restrictive: one could reasonably regard it as satisfied by any $X \gtrsim 10^{-1}$.

Appendix A. Levinson's theorem

For any given scattering channel there is generally a relation between the number n_b of bound states and the change $\delta(p=0)-\delta(p\to\infty)$ of the phase shift from threshold to infinity. In all the cases that concern us here, we can and do choose $\delta(p\to\infty)=0$, and shall talk simply of $\delta(0)$. In nonrelativistic potential theory the relation is called Levinson's theorem, and modern methods tend to prove it by using the analyticity properties of the S matrix, and of suitably defined solutions of the 3D Schrödinger equation (see, e.g., Goldberger and Watson (1964), Newton (1982)). The case of relativistic particles described by the Dirac equation is more subtle, and still under study (see, e.g., Calogeracos and Dombey (2004)); and as regards electromagnetic scattering the writer knows of no general results.

Nevertheless, one can gain some insight through more old-fashioned proofs of Levinson's theorem, which reason from the constancy of the number of states (the dimensionality of the Hilbert space) as the potential is switched on. The idea is that without the potential all states are in the continuous spectrum (positive energy), that any bound state is formed by a state moving down from positive to negative energy, and that this move changes $\delta(0)$ by π. For even-parity solutions of the 1D Schrödinger equation with a reflection-symmetric potential, such an argument (Barton 1985) yields

$$\delta^{(+)}(0)=\pi\left(n_b^{(+)}-1/2\right),\qquad\text{(1D Schrödinger equation, even parity)}. \tag{A.1}$$

It may be compared with the theorem for the partial-wave phase shifts in spherically symmetric potentials, which reads

$$\delta^{(l)}(0)=\pi n_b^{(l)},\qquad\text{(3D Schrödinger equation with spherical symmetry)}. \tag{A.2}$$

All we shall do here is to compare the actual behaviour of our TE and TM phase shifts with what might have been expected in the light of (A.1) or of (A.2). It seems natural to look for similarities between the 1D Schrödinger system and our Maxwell waves having given polarization and fixed $\mathbf{k}$. (For simplicity we do not pursue the peculiarities of the special case where $k=0$.) The outcome is surprising, and instructive if only as a caution against seeing analogies where none exist in fact; and also perhaps as an incentive for a systematic search for Levinson-type theorems applicable to electromagnetic scattering by materials of various kinds. Meanwhile, we merely consider some mathematical facts for the very special model under study: the poles of the TM amplitudes are also treated as mere facts, with no attempt to relate them *a priori* to the threshold behaviour of the phase shift μ, or to the existence of the surface modes.

Section 2.2 has noted that the TE phase shift specified by (2.16) obeys $\eta(p=0)=-\pi/2$. This tallies with (A.1) if we take $n_b^{\mathrm{TE},+}=0$, conformably with there being no TE bound modes. The correspondence is no accident. If one represents the TE fields through their Debye potentials ψ, say through

$$\mathbf{E}^{\mathrm{TE}}\sim\boldsymbol{\nabla}\times[\hat{\mathbf{z}}\exp(\mathbf{ik}\cdot\mathbf{s})\psi^{\mathrm{TE}}(z)], \tag{A.3}$$

(adapted to 1D from the 3D treatment given e.g. Bouwkamp and Casimir (1954), or Jackson (1975)), then ψ turns out to obey the same equation and the same matching conditions as the 1D Schrödinger wavefunction in the presence of a repulsive potential proportional to $\delta(z)$. Such a potential is well defined, and naturally lacks bound states. Since the equations are isomorphic, so are the solutions, and Levinson's theorem applies to TE as of right. The same is true in 3D (see B.III): the TE partial waves scattered from a spherical shell satisfy (A.2).

TM phase shifts behave quite differently. Equation (2.16) shows that $\mu(p=0,k\neq0)=0$, which cannot be made to tally with (A.1) for any integer value of n_b. This discrepancy reflects the fact, contrary to what uncritical inspection might suggest, that with respect to

dependence on energy or frequency the matching conditions for the TM Debye potential are by no means similar to those for a Schrödinger equation with a potential proportional to[11] $\delta'(z)$ (nor with any other local potential).

Finally, it is instructive to count states. Since μ is the same at $p = 0$ and at $p = \infty$ (namely zero), just as it would be in the absence of the sheet (when it vanishes identically at all p), the number of states in the TM continuum is also the same with the sheet as without. (To see this one discretizes the states as we did in section 3.3.1, and as for the proof of the 1D Levinson's theorem (Barton 1985).) It follows that the bound mode is *not* a continuum mode attracted below threshold by interaction with the sheet. Rather it must be counted *additionally* to the TM photon modes, as confirmed by its survival in the NR model (which is constructed from electrostatics with no reference to photons). Essentially the same physics operates for the 3D spherical shell, subject to the complication that in 3D the exact theory dissolves the bound modes of the NR model (B.IV) into the continuum. Thus the continuum of each exact TM partial wave contains *one more* state than it would in the absence of the shell. Correspondingly, the TM phase shifts in 3D obey a kind of anti-Levinson theorem: one finds $\delta_l^{\mathrm{TM}} = -\pi$, as if one had (A.2) with $n_b = -1$.

Appendix B. The nonretarded model

We adapt the theory elaborated in B.IV for a spherical shell, to construct a model with close similarities to Fetter's (1973) theory for a 2D Fermi gas. The model admits only nonretarded Coulomb forces: thus there is no B field, no photons, and the electric field is purely longitudinal:

$$\mathbf{E} = -\boldsymbol{\nabla}\Phi, \qquad \nabla^2\Phi(\mathbf{r}) = -4\pi\sigma(\mathbf{s})\delta(z - z'), \qquad \Phi(\mathbf{s}, |z| \to \infty) = 0,$$

where $\sigma = -ne\boldsymbol{\nabla}_\parallel \cdot \boldsymbol{\xi}$. Accordingly, Newton's second law reads

$$\ddot{\boldsymbol{\xi}} = -(e/m)\boldsymbol{\nabla}_\parallel\Phi \quad \Rightarrow \quad \boldsymbol{\xi}(s) \equiv -\nabla_\parallel\Psi(\mathbf{s}), \qquad \ddot{\Psi}(\mathbf{s}) = (e/m)\Phi(\mathbf{s}, z = 0), \tag{B.1}$$

with the displacement potential $\Psi(\mathbf{s})$ defined only on the sheet. Thus $\boldsymbol{\xi}$ is curl-free, and for any normal mode one has

$$\Phi_\omega \text{ and } \Psi_\omega \propto \exp(-\mathrm{i}\omega t) \quad \Rightarrow \quad \Psi_\omega(\mathbf{s}) = -(e/m\omega^2)\Phi_\omega(\mathbf{s}, z = 0), \tag{B.2}$$

$$\mathrm{discont}(\Phi) = 0, \qquad \mathrm{discont}\left(\frac{\partial\Phi_\omega}{\partial z}\right) = -4\pi\sigma = \frac{4\pi ne^2}{m\omega^2}\nabla_\parallel^2\Phi_\omega. \tag{B.3}$$

The energy is

$$\int \mathrm{d}^2s\,\frac{1}{2}nm\,\dot{\boldsymbol{\xi}}^2 + \frac{1}{2}\int\int \mathrm{d}^2s\,\mathrm{d}^2s'\,\frac{\sigma(\mathbf{s})\sigma(\mathbf{s}')}{|\mathbf{s} - \mathbf{s}'|} = \int \mathrm{d}^2s\left\{\frac{1}{2}nm\,\dot{\boldsymbol{\xi}}^2 + \frac{1}{2}\sigma\Phi\right\}. \tag{B.4}$$

The only normal modes are surface plasmons with frequency Ω_{NR} given by

$$\Omega_{\mathrm{NR}}^2 = 2\pi ne^2k/m = c^2qk, \tag{B.5}$$

where we have admitted the combination q from (2.5) because it permeates the properly retarded theory, even though in the nonretarded model c and q separately play no role.

[11] Worse, potentials proportional to $\delta'(z)$ in the Schrödinger equation are under-defined (unlike $\delta(z)$), a fact well known to but not very tellingly advertized by mathematicians. For instance, significantly different consequences follow depending on whether one treats $\delta'(z)$ as the limit of local or of separable representations (Barton and Waxman 1993). Worse still, in both cases the limit produces perfect reflection, i.e. $\mathcal{T} = 0$, *at all* p, incompatibly with (2.15).

To turn (B.4) into

$$H_{\rm NR} = \frac{\hbar}{2}\int \mathrm{d}^2k\,\Omega_{\rm NR}\big(a^\dagger_{\mathbf{k}}a_{\mathbf{k}} + a_{\mathbf{k}}a^\dagger_{\mathbf{k}}\big), \qquad \big[a_{\mathbf{k}}, a^\dagger_{\mathbf{k}}\big] = \delta(\mathbf{k}-\mathbf{k}'),$$

one quantizes with

$$\Phi = \int \mathrm{d}^2k \sqrt{\frac{\hbar\Omega_{\rm NR}}{4\pi k}}a_{\mathbf{k}}\exp\left(-\mathrm{i}\Omega_{\rm NR}t + \mathrm{i}\mathbf{k}\cdot\mathbf{s} - k\,|z|\right) + Hc. \tag{B.6}$$

The expansions of Ψ and of $\boldsymbol{\xi}$ then follow on setting $\omega \to \Omega_{\rm NR}$ in (B.1), (B.2).

Recall that sums per unit area are given by $\int \mathrm{d}^2k/(2\pi)^2 \ldots$. Thus the zero-point energy per unit area reads

$$\beta_{\rm NR} = \int_0^K \frac{2\pi\,\mathrm{d}k\,k}{(2\pi)^2}\frac{\hbar\Omega_{\rm NR}}{2} = \frac{\hbar c\sqrt{q}}{4\pi}\int_0^K \mathrm{d}k\,k^{3/2} = \hbar c\sqrt{q}\frac{K^{5/2}}{10\pi} = \frac{4\pi^{3/4}}{5}\hbar\sqrt{\frac{e^2}{ma^7}}. \tag{B.7}$$

Since the system is, in effect, a set of nonrelativistic oscillators, the standard virial theorem applies: the ground-state expectation values of the kinetic and of the potential energies, i.e. of the first and the second terms in (B.4), are each equal to $\beta_{\rm NR}/2$. The model is so simple that the conclusion is easily verified by direct calculation.

Appendix C. The integrals $\mathcal{H}_{\rm TE}$ and $\mathcal{H}_{\rm TM}$ in β

An integration by parts puts $\mathcal{H}_{\rm TE}$, as defined by (3.15), (3.17), into the form

$$\mathcal{H}_{\rm TE} = 1 - \frac{\pi y}{2} + \lim_{x\to\infty}\left\{\log\left(\frac{y}{2x}\right) + \int_0^x \mathrm{d}x'\frac{\sqrt{x'^2+y^2}}{(x'^2+1)}\right\}. \tag{C.1}$$

On rationalizing the integrand by changing the variable from x' to $\xi = \sqrt{x'^2+y^2} + x'$, this becomes manageable, and eventually yields (3.22).

For $\mathcal{H}_{\rm TM}$ as defined by (3.16), (3.17) one starts likewise with an integration by parts, and finds

$$\mathcal{H}_{\rm TM} = \int_0^\infty \mathrm{d}x\left\{\frac{\sqrt{x^2+y^2}(x^2-y^2)}{(x^2+y^2)^2+x^2} + \frac{1}{\sqrt{x^2+y^2}} - \frac{2x^2}{(x^2+y^2)^{3/2}}\right\}. \tag{C.2}$$

This too is best approached as an indefinite integral with a finite but very large upper limit, which afterwards is allowed to tend to infinity. The first term proves extraordinarily troublesome, least so if one uses complex partial fractions to re-express its integrand as

$$\sqrt{x^2+y^2}\left[\frac{y_2}{x^2+y_2^2} - \frac{y_1}{x^2+y_1^2}\right], \qquad y_{1,2} \equiv \frac{1}{2}(\sqrt{4y^2+1}\mp 1), \tag{C.3}$$

with extensive use of the relations[12]

$$y_2 - y_1 = 1, \qquad y_1y_2 = y^2, \qquad y^2 - y_1^2 = y_1, \qquad y_2^2 - y^2 = y_2. \tag{C.4}$$

Then, rationalizing the integrand by the same change of variable as for $\mathcal{H}_{\rm TE}$, one eventually arrives at

$$\mathcal{H}_{\rm TM} = 2 - \sqrt{y_2}\tanh^{-1}\left(\frac{1}{\sqrt{y_2}}\right) - \sqrt{y_1}\tan^{-1}\left(\frac{1}{\sqrt{y_1}}\right). \tag{C.5}$$

Finally, integration over y yields (3.24). (Unfortunately, it seems impossible to exploit the apparent kinship with the function $A(\zeta)$ from B.VI.)

[12] These are analogous to (3.19), in the sense that they reproduce it on replacing $(y, y_1, y_2) \to (X, X_1, X_2)$.

References

Ashcroft N W and Mermin N D 1976 *Solid State Physics* (New York: Holt, Rinehart and Winston) chapter 20
Barnett S M, Huttner B, Loudon R and Matloob R 1996 *J. Phys. B: At. Mol. Opt. Phys.* **29** 3763
Barton G 1985 *J. Phys. A: Math. Gen.* **18** 479
Barton G 2001a *J. Phys. A: Math. Gen.* **34** 4083
Barton G 2001b *J. Phys. A: Math. Gen.* **34** 5781
Barton G 2002 *Int. J. Mod. Phys.* A **17** 767
Barton G 2004a *J. Phys. A: Math. Gen.* **37** 1011, referred to as B.III
Barton G 2004b *J. Phys. A: Math Gen.* **37** 3725, referred to as B.IV
Barton G 2005 *J. Phys. A: Math. Gen.* **38** 3021, referred to B.VI
Barton G and Calogeracos A 1995 *Ann. Phys., NY* **238** 227 section 3 and appendix A
Barton G and Dombey N 1985 *Ann. Phys., NY* **162** 231
Barton G and Waxman D 1993 Wave equations with point-support potentials having dimensionless strength parameters *Sussex Report*
Bordag M, Mohideen U and Mostepanenko V M 2001 *Phys. Rep.* **353** 1
Bouwkamp C J and Casimir H B G 1954 *Physica* **20** 539
Boyer T H 1968 *Phys. Rev.* **174** 1764
Calogeracos A and Dombey N 2004 *Phys. Rev. Lett.* **93** 180405
Fetter A L 1973 *Ann. Phys., NY* **81** 367
Genet C, Lambrecht A and Reynaud S 2003 *Phys. Rev.* A **67** 043811
Goldberger M L and Watson K M 1964 *Collision Theory* (New York: Wiley)
Graham N, Jaffe R L, Khemani V, Quandt M, Schröder O and Weigel H 2004 *Nucl. Phys.* B **677** 379
Huttner B and Barnett S M 1992 *Phys. Rev.* A **46** 4306
Jackson J D 1975 *Classical Electrodynamics* 2nd edn (New York: Wiley)
Marachevsky V N 2001a *Phys. Scr.* **64** 205
Marachevsky V N 2001b *Mod. Phys. Lett.* A **16** 1007
Newton R G 1982 *Scattering Theory of Waves and Particles* 2nd edn (New York: Springer)
Reynaud S, Lambrecht A and Genet C 2004 *Quantum Field Theory under the Influence of External Conditions* ed K A Milton (Paramus, NJ: Rinton) (*Preprint* quant-ph/0312224)
Robaschik D and Wieczorek E 1994 *Ann. Phys., NY* **236** 43
Suttorp L G and Wubs M 2004 *Phys. Rev.* A **70** 013816